Microstructural Insights into the Transformation of Cubic, Low-Temperature, Disordered Cu_2ZnSnS_4 into the Tetragonal Form

S. Bette[a,*], E. Isotta[b, §,*], B. Mukherjee[b,$,*], A. Schulz[a], Z. Dallos[c], U. Kolb[c], Robert E. Dinnebier[a], P. Scardi[b]

[a]Max Planck Institute for Solid State Research**,** Heisenbergstr. 1, 70569 Stuttgart (Germany)

[b]Department of Civil, Environmental & Mechanical Engineering, University of Trento, via Mesiano 77, 38123, Trento (Italy)

[c]Johannes Gutenberg-Universität MainzDuesbergweg 10-14, 55128 Mainz, Germany

§: E. Isottsa: Department of Materials Science and Engineering, Northwestern University, 2220 Campus Drive, 60208 Evanston (USA). Email: Eleonora.isotta@gmail.com.

$: B. Mukherjee: current affiliation: Materials Research and Technology Department, Luxembourg Institute of Science and Technology (LIST), Avenue des Hauts-Fourneaux 5, L-4362, Esch/Alzette, Luxembourg. Email: binayak.mukherjee@list.lu.

Additional Graphics and Tables

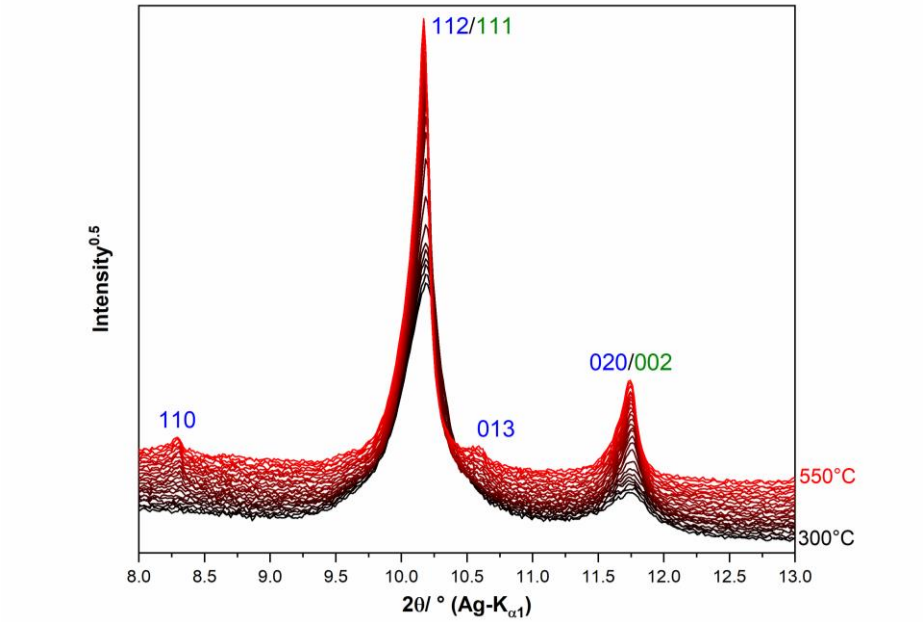

Figure S 1. Excerpt of the *in situ* XRPD patterns recorded during the heating of CZTS (Figure 3 a) including selected reflection indices for the cubic (green font color) and the tetragonal cell (blue font color).

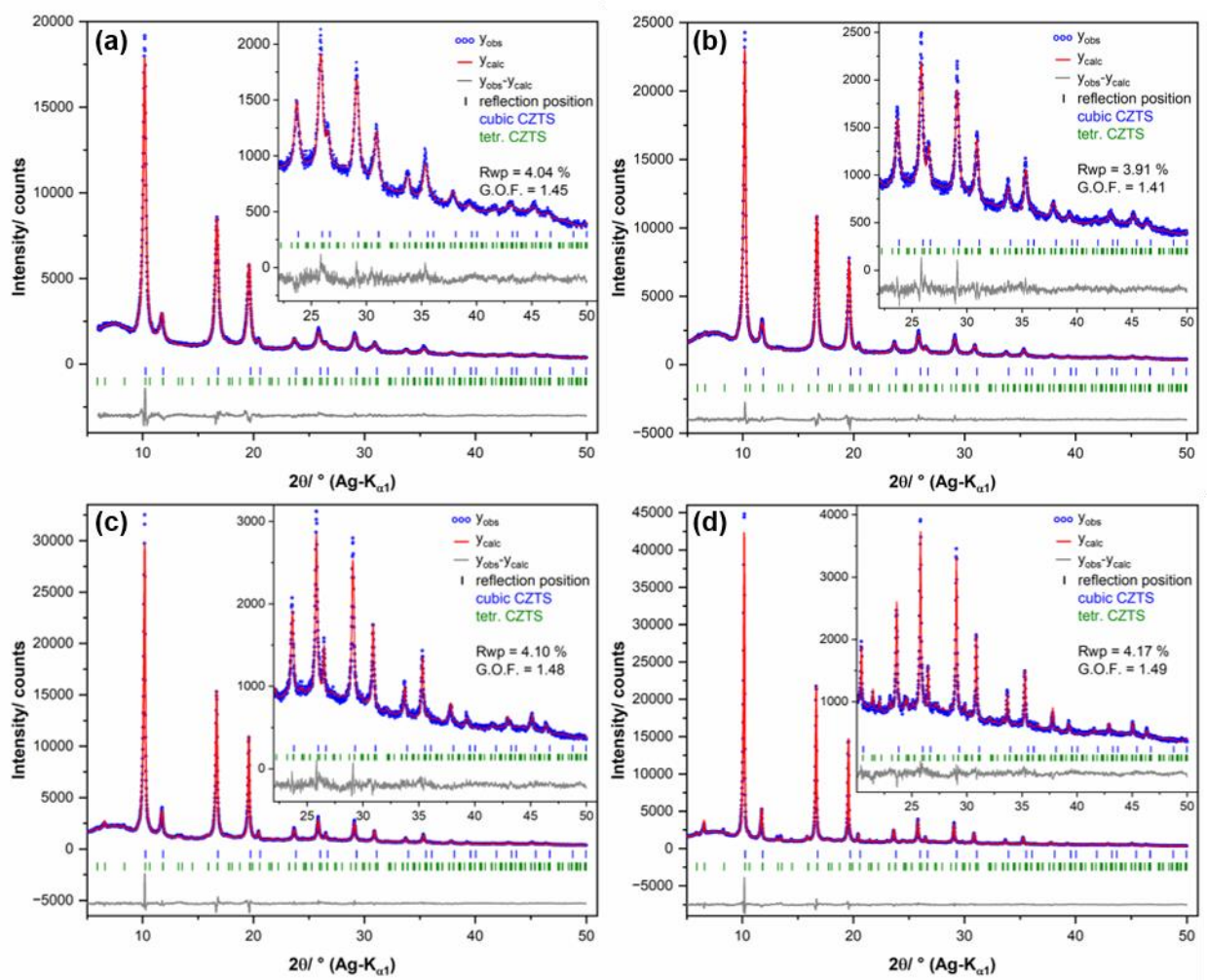

Figure S 2. Graphical results of the final Rietveld refinement of XRPD patterns recorded during the heating of WC-milled CZTS collected at (a) 300 °C, (b) 360 °C, (c) 380 °C, (d) 500 °C. The high angle parts of the patterns are enlarged by a factor of 8-10 for clarity (insets).

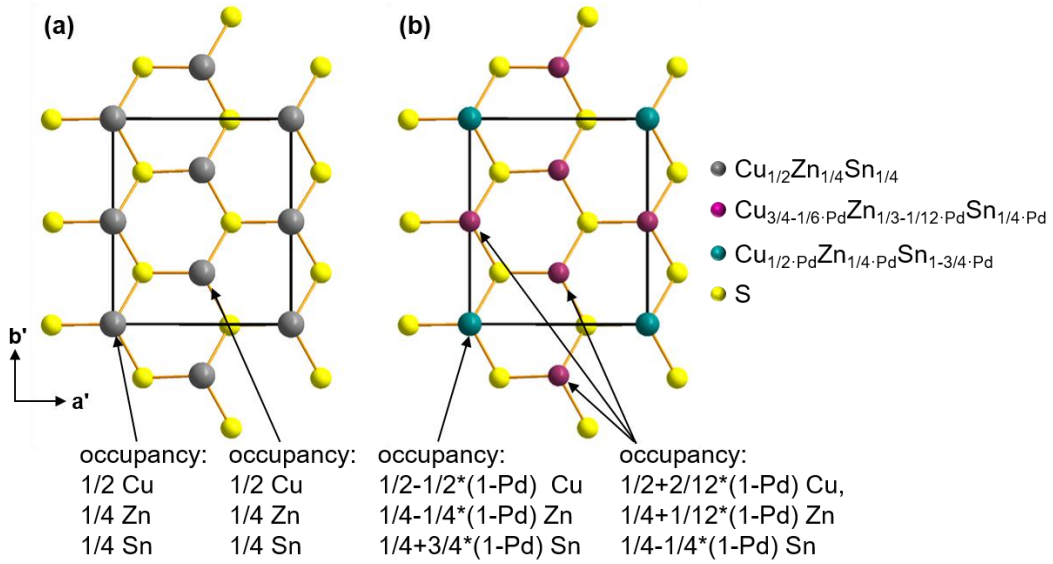

Figure S 3. Topview on the layer setup of CZTS used for the refinement of the temperature dependent in situ XRPD data. The ordering of the tin cations was modelled by increase the tin occupancy at (0, 0, 0) and decreasing its occupancy on all other metal positions accordingly using the tin disorder-parameter Pd, with Pd = 0 → full tin ordering and Pd = 1 → full tin disorder.

Table S 1. Atomic coordinates of layers used for the refinement of stacking faulted CZTS employing space group P1, a' = 6.6527 Å, b' = 7.6819 Å, c' = N*18.78 Å and α' = β' = γ' = 90 ° at room temperature.

atoms	**x**	**y**	**z**
Sn/Cu/Zn1a	0	0	0
Sn/Cu/Zn1b	0.5	0.25	0
Sn/Cu/Zn1c	0.5	0.75	0
Sn/Cu/Zn1d	0	0.5	0
S1a	0.3333	0	-0.0427
S1b	0.3333	0.5	-0.0427
S1c	0.8333	0.25	-0.0427
S1d	0.8333	0.75	-0.0427
Stacking vector	2/3	0.5	1/6

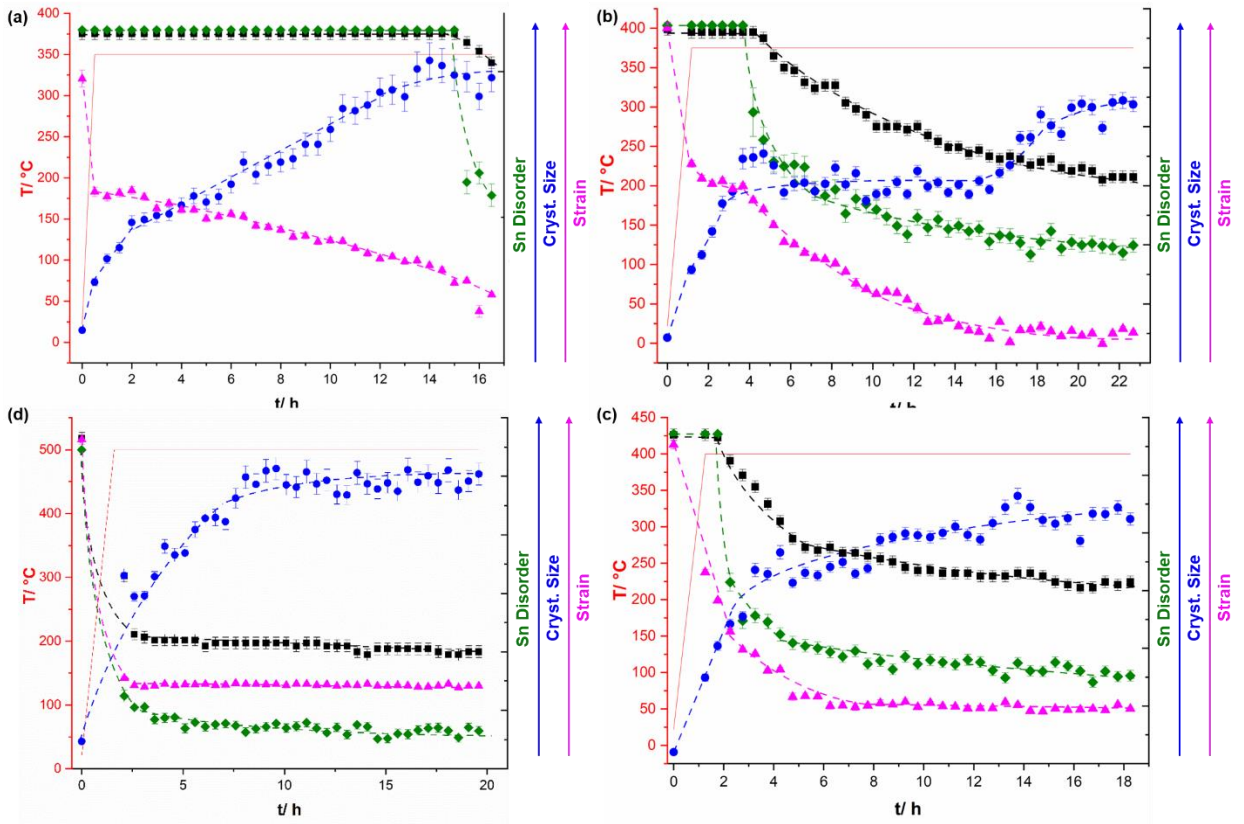

Figure S 4. Results of the XRPD analyses of isothermal heating experiments of CZTS at (a) 350 °C, (b) 375 °C, (c) 400 °C and (d) 500 °C.

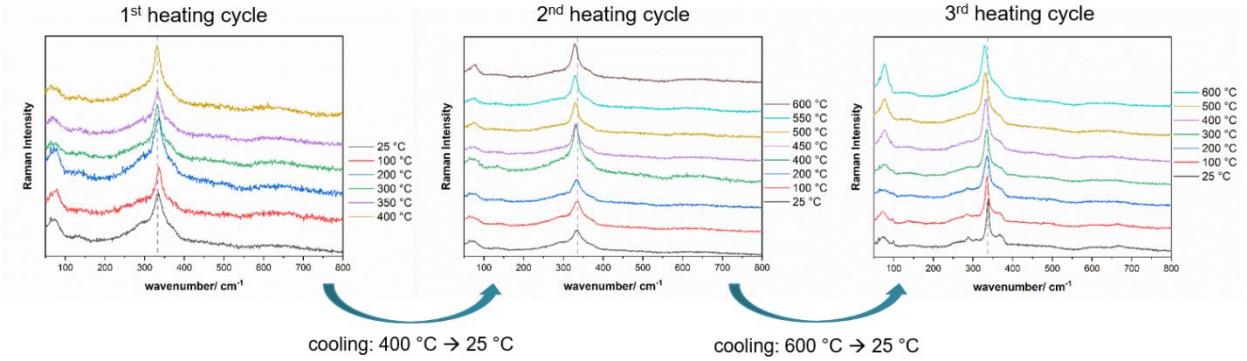

Figure S 5. Temperature dependent in situ Raman spectra of WC-milled, cubic, disordered kesterite applying a circular heating profile where the sample was heated up to 400 °C and subsequently cooled to room temperature during the first and second heating cycle. During the last heating cycle the samples was heated up to 600 °C.

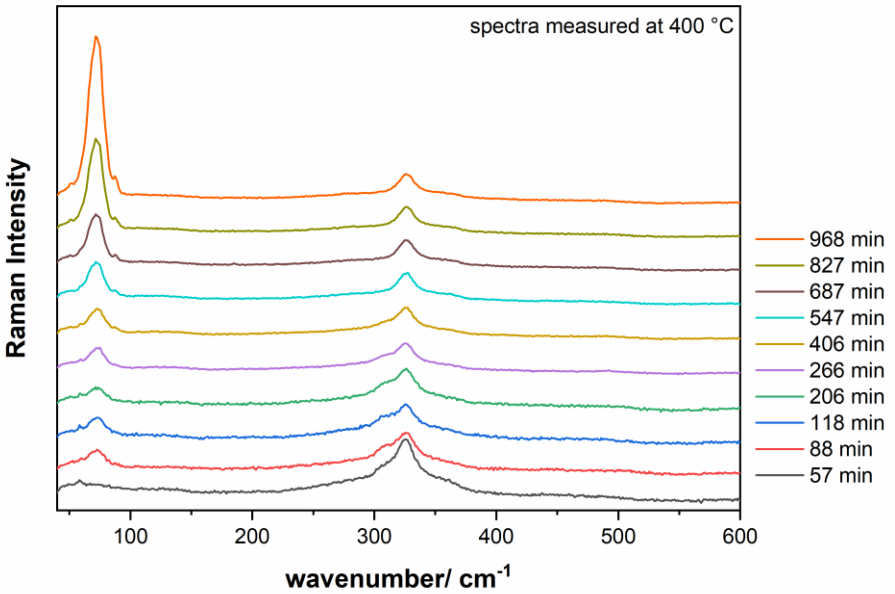

Figure S 6. Temperature dependent *in situ* Raman spectra, recording during the isothermal heating of disordered cubic kesterite at 400 °C, reached after 57 minutes of heating.

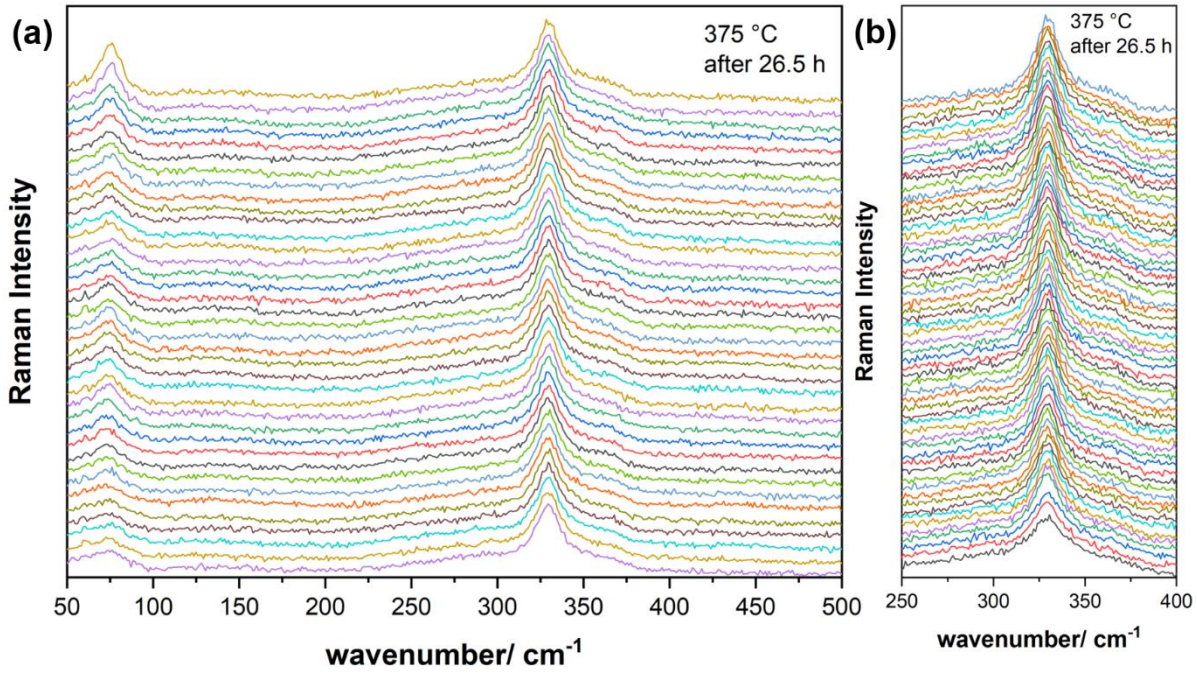

Figure S 7. (a) Temperature dependent *in situ* Raman spectra, recording during the isothermal heating of disordered cubic kesterite at 375 °C, the excerpt (b) illustrates the sharpening of the Raman band at 332 cm^{-1}.

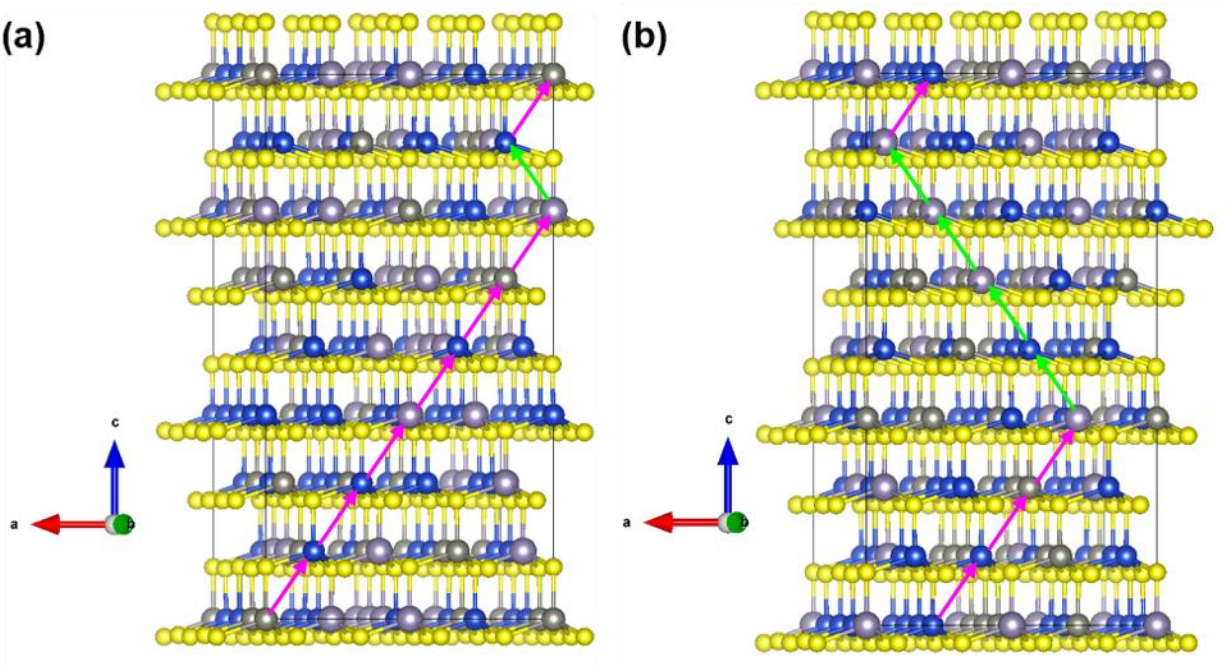

Figure S 8. Simulation supercell models for CZTS with (a) a dislocation fault and (b) a twin fault. Stacking vectors are indicated by magenta and green arrows.

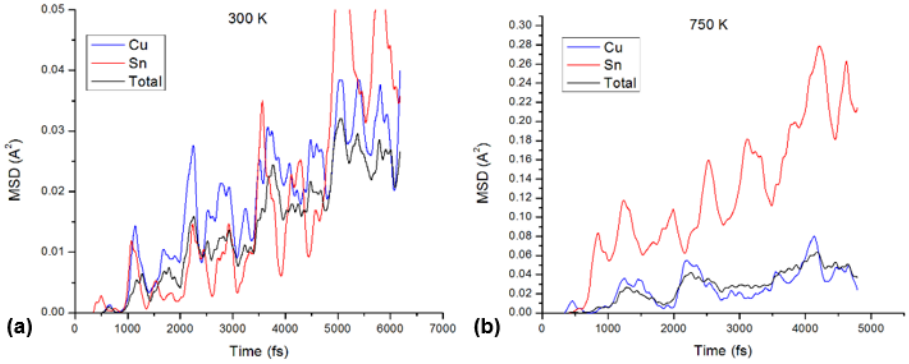

Figure S 9. Evolution of the mean square displacements for cubic CZTS (a) below and (b) above the phase transition temperature, showing the increased mobility of Sn.